Canadian Mineralogist
Vol. 23, pp. 111-127 (1985)

RELATIONSHIPS BETWEEN TEMPERATURE AND OXYGEN FUGACITY AMONG Fe–Ti OXIDES IN TWO REGIONS OF THE DULUTH COMPLEX

JILL DILL PASTERIS
Department of Earth and Planetary Sciences and McDonnell Center for Space Sciences, Washington University, Box 1169, St. Louis, Missouri 63130 U.S.A.

ABSTRACT

Fe–Ti-oxide minerals from about 20 sulfide-oxide-mineralized samples from the South Kawishiwi (Inco) and Partridge River (Minnamax) troctolitic intrusive bodies of the Duluth Complex were studied by microscopy and electron-microprobe analysis. At Minnamax, ilmenite (Ilm) occurs almost to the exclusion of magnetite (Mt), whereas the association of Mt and Ilm is common at Inco. Compositions of Mt–Ilm pairs were plotted on T–$f(O_2)$ diagrams. As is common in slowly cooled gabbroic bodies, the Mt–Ilm pairs show varying degrees of re-equilibration to subsolidus temperatures (~ 650 to 850°C), thus depicting the T–$f(O_2)$ trajectory as the rocks cooled. The Mt–Ilm pairs from Inco cluster around the QFM buffer curve for 1.5 kbar total pressure. The earliest oxide phases apparently formed at conditions somewhat more reducing than QFM, whereas later, intercumulus grains are more oxidized. The Fe^{3+} content of isolated grains of ilmenite from both bodies indicates that ilmenite at Amax represents a lower $f(O_2)$ value (1.5 log units at 800°C) than that at Inco, at all reasonable temperatures. Thus, the oxide data confirm the previous interpretation inferred from the sulfide mineralogy, that the $f(O_2)$ was lower in the Partridge River than in the South Kawishiwi complex. The same relative difference of oxygen fugacity is suggested by gas-chromatography – mass-spectrometry analyses on trapped volatiles in bulk-rock samples. This has implications for the mechanism of Cu–Fe–Ni-sulfide segregation, which is $f(O_2)$-dependent. The $f(O_2)$ and $f(S_2)$ values calculated from the composition of the coexisting oxide and sulfide phases permit an estimation of conditions in the melt during sulfide precipitation. As has been indicated in previous studies, assimilation of country rock (Virginia Formation) probably was essential to the development of an immiscible sulfide liquid in several regions of the Duluth Complex. The present work emphasizes the importance of the assimilation of not only sulfur, but also reducing materials, to produce a moderate $f(O_2)$ conducive to sulfide immiscibility.

Keywords: sulfide immiscibility, Duluth Complex, Fe–Ti oxides, geothermometry, oxygen barometry, Cu–Fe–Ni sulfides, Minnesota.

SOMMAIRE

On a étudié, au microscope et à la microsonde électronique, les oxydes de Fe–Ti d'environ 20 échantillons minéralisés en sulfures et oxydes des massifs troctolitiques de Kawishiwi du Sud (Inco) et de Partridge River (Minnamax) du complexe de Duluth. A Minnamax, l'ilménite (Ilm) se présente presque sans magnétite (Mt), alors que l'association Mt + Ilm est courante à Inco. On a porté les compositions des paires Mt–Ilm sur le diagramme T – $f(O_2)$. Comme cela se voit souvent dans les complexes gabbroïques refroidis lentement, les paires Mt–Ilm montrent, à des degrés divers, leur rééquilibration à une température subsolidus (d'environ 650 à 850°C), traçant ainsi la trajectoire de T – $f(O_2)$ au cours du refroidissement. Les paires Mt–Ilm de Inco se groupent autour de la courbe du tampon QFM à une pression total de 1.5 kbar. Les premières phases d'oxyde semblent s'être formées dans des conditions un peu plus réductrices que le tampon QFM, alors que les phases intercumulus ultérieures sont plus oxydées. D'après le contenu en Fe^{3+} des grains d'ilménite séparés des deux massifs, il appert que l'ilménite d'Amax représenterait une valeur de $f(O_2)$ (1.5 unités log à 800°C) inférieure à celle de l'ilménite d'Inco, à toute température raisonnable. Ainsi, l'étude des oxydes confirme les interprétations antérieures, fondées sur la minéralogie des sulfures, à savoir que la fugacité d'oxygène était plus faible à Partridge River qu'à Kawishiwi. La même différence relative en fugacité d'oxygène est indiquée par chromatographie en phase gazeuse et par spectrométrie de masse sur les éléments volatils inclus dans les échantillons de roche globale. De ces observations découlent des implications sur le mécanisme de ségrégation des sulfures de Cu–Fe–Ni, qui dépend de $f(O_2)$. Les valeurs de $f(O_2)$ et de $f(S_2)$ calculées à partir des compositions des phases coexistantes d'oxyde et de sulfure permettent d'évaluer les conditions du magma au cours de la précipitation des sulfures. Comme l'indiquaient des études antérieures, l'assimilation de la roche encaissante (formation de Virginia) fut sans doute essentielle au développement d'un liquide sulfuré immiscible, dans plusieurs régions du complexe de Duluth. Cette étude souligne l'importance de l'assimilation non seulement du soufre, mais aussi de matériaux réducteurs, pour produire une $f(O_2)$ moyenne favorable à l'immiscibilité des sulfures.

(Traduit par la Rédaction)

Mots-clés: immiscibilité des sulfures, complexe de Duluth, oxydes de Fe–Ti, géothermométrie, barométrie de l'oxygène, sulfures de Cu–Fe–Ni, Minnesota.

INTRODUCTION

In an overview investigation of oxide–sulfide–silicate relationships in the Duluth Complex, approximately 20 samples of sulfide-mineralized drill core and hand samples from the Inco mine site and the Minnamax prospect (presently owned by Ken-

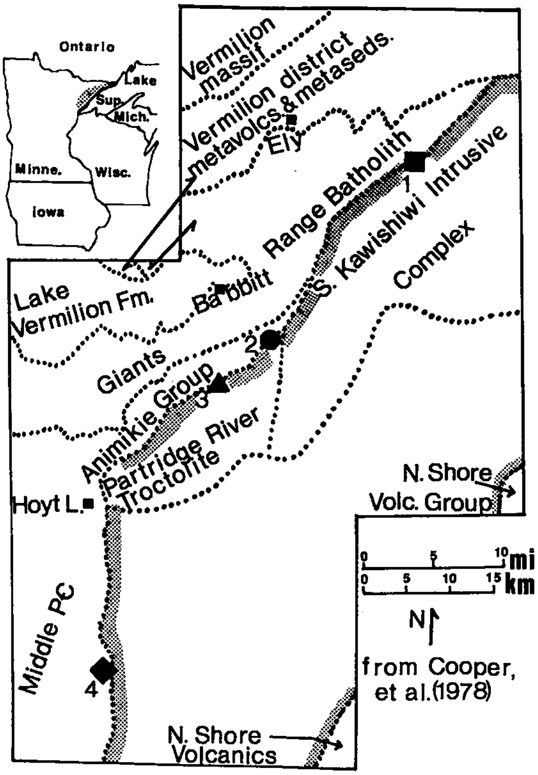

FIG. 1. Index map and geologic sketch map of the Duluth Complex region (after Cooper *et al.* 1978). The numbered localities are: 1 Inco mine site, 2 Minnamax prospect, 3 U.S. Steel prospect, and 4 Water Hen intrusive body. Extent of the Duluth Complex designated by shaded border.

necott) were studied (Fig. 1). The material from Inco (provided by M. Boucher) represents troctolite and augite-bearing troctolite from a section of the South Kawishiwi intrusive body near the site of the Inco shaft (see Cooper *et al.* 1978 and Fig. 1 of this paper). The Minnamax samples come from part of the adjacent Partridge River troctolitic body, and are macroscopically similar to the Inco material. These are documented drill-core samples from Hole 146 in the southern end of the Tiger Boy deposit (Watowich 1978), and come from depth levels 173 to 586 metres (provided by S. Watowich, Amax). The dominant rock-type is troctolite, but a hornfels zone also was sampled; it may represent xenoliths of underlying metasedimentary and metavolcanic rocks.

These particular samples were chosen from the two areas because they are representative of the range of sulfide mineralization, as described by Pasteris (1984). The accompanying opaque oxide phases, predominantly magnetite and ilmenite, are the focus of the present study. Sample numbers are the same as those referred to in Pasteris (1984). DG prefixes designate Inco samples; 146 prefixes designate Minnamax samples.

Previous work

Several studies have been published on the sulfide mineralogy (Weiblen & Morey 1976, Boucher 1975, Pasteris 1984) and the general geological relationships of the sulfide deposits in the Duluth Complex, northeastern Minnesota (*e.g.*, Bonnichsen 1972a, 1974, Tyson & Chang 1984). More recently, results of oxygen and sulfur isotope analyses have been interpreted for the Dunka Road deposit (Ripley & Rao 1980, Ripley 1981, Rao & Ripley 1983); rubidium–strontium isotope analyses also have been done on a Minnamax drill core (Grant & Molling 1981). Both rock suites come from the Partridge River troctolite. Mainwaring & Naldrett (1977) carried out sulfur isotope analyses on the Cu–Ni-mineralized Water Hen intrusive body to the south (Fig. 1).

The general conclusion of these studies is that reactions between the igneous melt(s) and the surrounding country-rock may have strongly affected the precipitation of sulfide phases in the Duluth Complex. Questions still remain regarding the physical mechanism of this interaction (probably a type of volatile distillation rather than large-scale bulk assimilation: Grant & Molling 1981, Ripley 1981). It is also unclear exactly how the interaction affected the timing of sulfide precipitation and the specific compositions of the various segregations of sulfide that formed in the troctolite intrusive bodies. The textures and mineral assemblages indicate that an immiscible sulfide melt developed during intercumulus precipitation. However, some pyrrhotite segregations have been partly or totally replaced by cubanite ± chalcopyrite. Pasteris (1984) therefore concluded that the present sulfide mineralogy is a product of both the immiscibility of a sulfide melt and its subsequent interaction with a metal-enriched (mainly Cu-bearing) mobile fluid. Rao & Ripley (1983) postulated as an alternative, the development of a late-stage, Cu-rich sulfide melt, which produced Cu-sulfide-rich zones in the troctolite.

In the more recent studies on the Duluth Complex (*e.g.*, Ripley & Rao 1980, Ripley 1981, Rao & Ripley 1983), increasing emphasis has been placed on the interpretation of the sulfide concentrations in the context of the entire mineral-assemblage. One important aspect of the petrology and petrography that has not been investigated in detail is the mineralogy of the opaque oxide phases. Bonnichsen (1972b), Phinney (1972) and Hardyman (1969) briefly described several types of occurrences of oxide phases, and Hardyman (1969) and Weiblen & Morey (1980) presented electron-microprobe data for several grains of ilmenite.

The goal of the present study is the analysis and interpretation of the Fe–Ti oxides in selected samples from the South Kawishiwi (Inco) and Partridge River (Minnamax) intrusive complexes. One aim is to confirm or refute an earlier interpretation, primarily founded on the sulfide assemblages, that the Inco deposit formed under relatively more oxidizing conditions than those at Amax (Pasteris 1984). This interpretation was based on 1) the occurrence of the stoichiometric iron sulfide phase *troilite* at Amax, in contrast to hexagonal pyrrhotite in most Inco samples, and 2) the occurrence of very fine-grained graphite (presumably vapor-deposited) in veinlets at Amax but not at Inco. From the data on the oxides, temperature - oxygen fugacity paths are inferred for the cooling of the two bodies. The similarities and differences in the oxide relationships are examined and related to the distinctive sulfide assemblages. Some aspects of sulfide immiscibility in the troctolites are interpreted in light of the $f(S_2)$ and $f(O_2)$ values inferred from the coexisting oxide and sulfide phases.

PETROGRAPHY OF OXIDE PHASES

Opaque oxide phases are common constituents in both the Amax and Inco suites. The most common minerals are ilmenite and magnetite, but small amounts of other spinels also occur. There is no one-to-one correlation between the abundances of the sulfides and oxides, but the samples with the highest oxide concentrations usually have the most sulfides. Samples from both Amax and Inco contain up to several modal % oxides, the most concentrated samples usually containing the coarsest oxide grains. Most specimens analyzed in this study contain at least 1–2 modal % oxides. It should be recognized, however, that the sample suites are biased toward sulfide-bearing rocks.

The overall textural features of the two suites are very similar. In terms of the mineralogy of the sulfide and oxide phases, however, the Amax and Inco occurrences differ (Pasteris 1984; Table 1, this paper). Firstly, the textural types will be described, and then the two petrological types will be distinguished.

In both suites, opaque oxides occur as (1) coarse blebby to lath-shaped grains, in some cases exceeding 4 mm (Fig. 2); (2) small ($\ll$1 mm), irregular to blebby bodies associated with intercumulus silicates (such as plagioclase, augite, biotite) and sulfides (Fig. 2) as well as enclosed in cumulus silicates; and (3) rodlets (10–50 μm) and extremely fine needles ($\sim 3 \times 10$ μm) within plagioclase and augite.

The large grains of type 1 appear to be coarse, intercumulus phases. They commonly are surrounded by several individual silicate grains, some of which lie in embayments or are fully enclosed within the oxide (Fig. 2). Bonnichsen (1972b) described the oxides as predominantly interstitial to plagioclase and olivine, but apparently contemporaneous with pyroxene. Large grains of ilmenite of type 1 usually appear optically continuous, as recognized by their anisotropism. However, several of the largest ones (>3 mm) are coarsely polycrystalline, perhaps because of partial recrystallization. Type-1 grains include monomineralic ilmenite and magnetite as well as coarse magnetite–ilmenite intergrowths; all exhibit the same textural relationships with the silicate phases. The coarse grains of oxide commonly are associated with mono- or polymineralic sulfides, with which they share straight or gently curved mutual boundaries (Fig. 3) Round blebs of sulfides (pyrrhotite, pentlandite, ± chalcopyrite) may be enclosed in the oxides (Fig. 4). Some cross-cutting sulfides are observed, and locally sulfides embay and apparently replace coarse oxides (Fig. 2).

Smaller grains of oxide of type 2 occur isolated in the core of cumulus silicates (especially augite and plagioclase; Fig.5), in the apparent adcumulus rims on cumulus silicates (Fig. 5), and as intercumulus granular intergrowths of oxides, sulfides and silicates (Fig. 6). The small, irregular inclusions within cumulus grains do not appear to be crystallographically oriented or to lie along growth zones. The type-2 intercumulus oxides commonly have textures that

TABLE 1. OXIDE OCCURRENCES, DULUTH COMPLEX

Deposit	Spinel & ilmenite lamellae in plag. & clinopyroxene	Large, separate ilmenite grains	Large, separate magnetite grains	Granular ilmenite-magnetite	Lamellar ilmenite in magnetite
Inco	abundant; usually concentrated at cores of cumulate grains	some; predominantly as laths within clinopyroxene	some: frequently with spinel and ilmenite exsolution lamellae	abundant; some probably primary some probably granular exsolution	abundant; apparently oxidation-exsolution
AMAX	abundant; usually concentrated at cores of cumulate grains.	abundant; some exceeding 3 mm; intercumulates	very rare; only in #146-1176	very rare; only in #146-1176	none observed

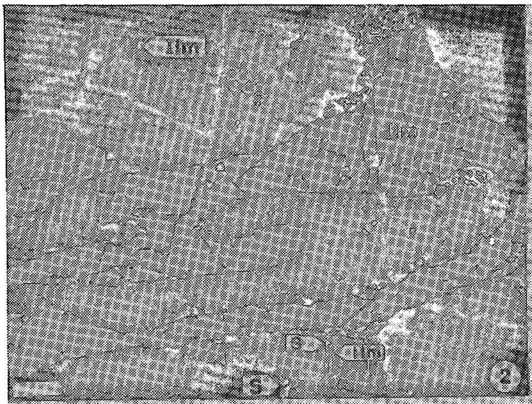

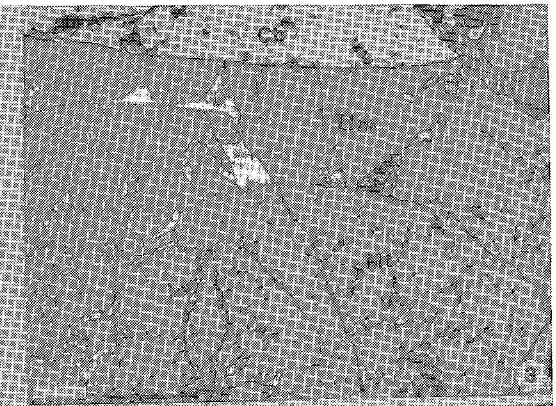

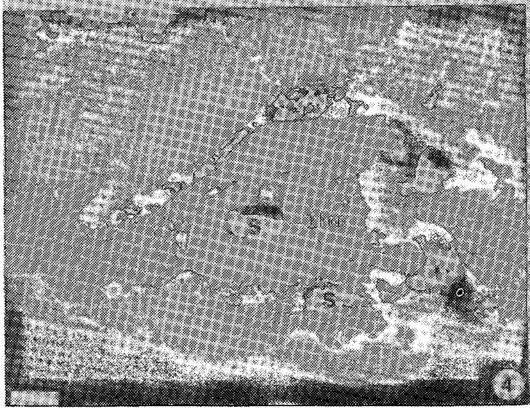

FIG. 2. Large, lamellar and small, irregular intercumulus grains of ilmenite (Ilm) surrounded by several grains of clinopyroxene and plagioclase. White sulfides (s) accompany and, in some cases, crosscut the ilmenite. DG-8, Inco. Scale bar 0.5 mm. Reflected light.

FIG. 3. Mutual grain-boundaries between coarse cubanite (Cb), ilmenite (Ilm), and magnetite (Mt). The oxide intergrowths probably arose from oxidation–exsolution. The magnetite contains minute inclusions (not visible in photograph) of spinel and ilmenite. DG-7, Inco. Scale bar 0.1 mm. Reflected light.

FIG. 4. Ilmenite (Ilm) and sulfide (S) grains, apparently contemporaneous, surrounded by plagioclase and some biotite. 146-1832, Minnamax. Scale bar 0.5 mm. Reflected light.

FIG. 5. Adjacent cumulate augite (A) and plagioclase (P). Fine lamellae of oxide (-l) occur in the early cumulus core of both silicates, but not in the adcumulus rim (-c). Blebby oxide and sulfide grains (black) have a lamella-free halo. DG-8, Inco. Scale bar 0.2 mm. Transmitted light.

closely mimic those of the associated sulfides, suggesting contemporaneity (Fig. 6).

In contrast to the above, the finest laths of oxide (type 3) are oriented in one or, less commonly, two directions in many augite and plagioclase grains. They are much less abundant in olivine grains. The rodlets characteristically are concentrated in the core of grains, suggesting that they delineate the region of cumulus growth (Pasteris 1984; Fig. 5, this paper). The adjacent intercumulus silicates usually contain no rodlets. In addition, in plagioclase and augite grains filled with fine oriented laths of oxide (type 3), there is usually a lath-free halo a few tens of micrometres wide around the coarser inclusions of type-2 oxide (Fig. 5).

Optical identification of the rodlets is difficult. Bonnichsen (1972b) found only ilmenite, whereas Phinney (1972) reported both ilmenite and magnetite in augite. Microprobe analysis in the present study has revealed magnetite, ilmenite, spinel (*sensu stricto*) and intergrowths of oxide phases. Spinel grains are very abundant. In transmitted light, they are recognized as medium brown platelets projecting downward from the thin-section surface. These oriented laths may have exsolved from their host silicates. Similar occurrences have been reported from several

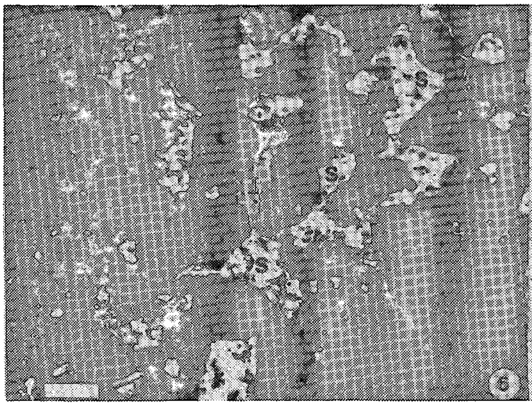

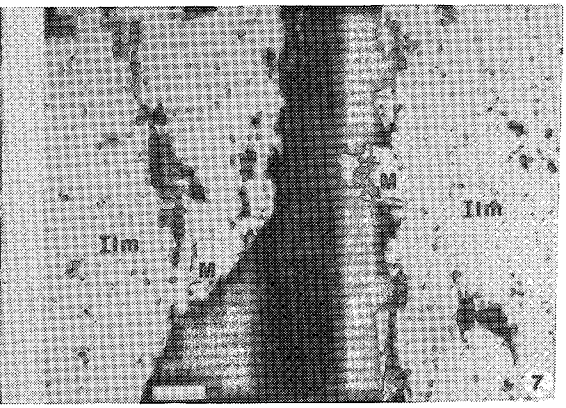

FIG. 6. Cubanite (white; S) and ilmenite (medium grey; I) appear to be contemporaneous intercumulates; associated with olivine and (bordering) plagioclase lath. 146–1787, Minnamax. Scale bar 0.1 mm. Reflected light.

FIG. 7. Large, lamellar intercumulus ilmenite (Ilm) grains generally are rimmed by granules of magnetite (whiter; M), which in turn contain black, oriented lamellae of spinel. The ilmenite-magnetite intergrowths probably resulted from oxidation–exsolution, whereas the spinel lamellae in the magnetite are of true exsolution origin. DG–8, Inco. Scale bar 50 μm. Reflected light, oil immersion.

gabbros (Garrison & Taylor 1981) and ultramafic rocks (*e.g.*, Salt Lake Crater xenoliths from Hawaii: White 1966, Pasteris, unpubl. data).

As indicated in Table 1, although all three textural types of oxides do occur in both suites, there is a distinct mineralogical difference between them. Both magnetite and ilmenite occur at the Inco site, but the oxide phase in the Amax samples is almost exclusively ilmenite (with very rare magnetite).

It is unclear simply from visual observation whether the coarse granular intergrowths of ilmenite and magnetite (Fig. 3) in the Inco suite are primary coprecipitates or the result of granular exsolution and recrystallization during oxidation–exsolution of an earlier titaniferous magnetite phase (*e.g.*, Lindsley 1976, Haggerty 1976). In contrast, large ilmenite grains like those in Figure 7 appear to be primary, whereas oriented intergrowths of lamellar ilmenite in magnetite (Fig. 8) are clearly suggestive of oxidation–exsolution. Within the latter magnetite host is also a fine-scale latticework (Fig. 8) of ilmenite lamellae (5–10 μm wide) and Mg–Al-spinel. These almost certainly represent oxidation–exsolution (ilmenite) and true exsolution (spinel) from an earlier titaniferous magnetite. The two scales of intergrowths suggest that the samples underwent two stages of oxidation–exsolution, the earlier one having produced the coarser lamellae of ilmenite. This is typical of slowly cooled intrusive bodies (*e.g.*, Haggerty 1976, Bowles 1977). In a subsequent section, compositional data are presented for the different occurrences of oxides.

Ilmenite is the major oxide phase in the Amax drill-core samples, and it also demonstrates the three textural types described above. In addition to the oriented minute laths (type 3) in silicates, there are somewhat larger blades of ilmenite, on the order of 0.8 mm, within plagioclase or interstitial to plagioclase laths. Some of the coarsest grains of ilmenite from Amax show rare, apparently stress-related twins (*cf.* Bonnichsen 1972b). The inclusion of oxide grains within large, subhedral laths of biotite is more common at Amax than at Inco (*cf.* Fig. 4).

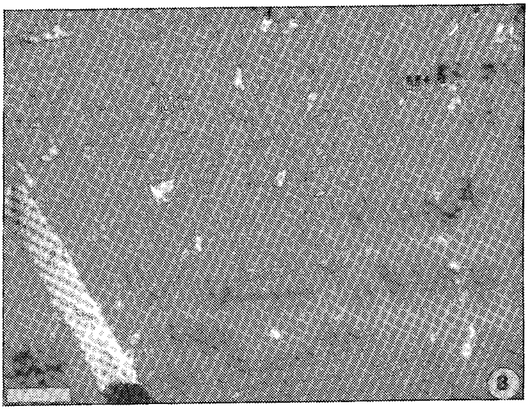

FIG. 8. Light grey titanomagnetite host (Mt) with oriented, coarse lamellae of medium-grey ilmenite (Ilm) and oriented, fine lamellae of black spinel. Spinel lamellae also occur in the ilmenite. The intergrowths are the products of oxidation–exsolution and true exsolution from an originally more titaniferous magnetite. DG–7, Inco. Scale bar 30 μm. Reflected light, oil immersion.

TABLE 2. COMPOSITIONS OF COEXISTING ILMENITE AND MAGNETITE

	#1A (4)	#1B (3)	#2A (4)	#2B (4)	#2C (4)	#3A (3)	#3B (1)	#4A (3)	#4B (3)
MgO	0.61	0.16	2.57	1.49	2.96	0.87	0.13	2.22	0.86
FeO	43.03	37.21	41.09	37.66	41.22	39.56	33.45	40.54	39.23
MnO	0.77	0.20	0.57	0.34	0.49	0.90	0.10	0.48	0.40
CaO	0.02	0.03	0.0	0.0	0.01	0.17	0.16	0.02	0.04
Al_2O_3	0.01	1.78	0.08	6.46	0.02	1.04	1.48	0.03	4.60
Cr_2O_3	0.01	0.07	0.33	15.37	0.25	0.56	2.43	0.12	6.16
Fe_2O_3	6.24	56.45	4.49	31.06	3.39	9.19	60.94	7.46	41.38
TiO_2	49.88	6.03	51.28	8.23	52.20	46.77	2.16	50.09	8.77
SiO_2	0.03	0.09	0.11	0.04	0.05	0.15	0.21	0.01	0.29
Total	100.60	102.02	100.52	100.31	100.59	99.21	101.06	100.97	100.73
Cation proportions, normalized to 3 (ilm) or 4 (mt) oxygen atoms									
Mg	0.023	0.009	0.095	0.080	0.108	0.033	0.007	0.082	0.046
Fe^{2+}	0.904	1.155	0.847	1.134	0.847	0.835	1.031	0.845	1.189
Mn	0.016	0.006	0.012	0.010	0.010	0.019	0.003	0.010	0.012
Ca	0	0.001	0	0	0	0.005	0.006	0.001	0.002
Al	0	0.078	0.002	0.274	0.001	0.031	0.065	0.001	0.196
Cr	0	0.002	0.006	0.438	0.005	0.011	0.072	0.002	0.177
Fe^{3+}	0.113	1.577	0.084	0.841	0.064	0.175	1.765	0.152	1.129
Ti	0.943	0.168	0.951	0.223	0.965	0.888	0.061	0.936	0.239
Si	0.001	0.003	0.003	0.001	0.001	0.004	0.008	0	0.010
Total	2.00	3.00	2.00	3.00	2.00	2.00	3.00	2.00	3.00
Recalculated as Ilmenite (Fe^{2+}), Geikielite (Mg), Hematite (Fe^{3+}) <u>or</u> Magnetite (Fe^{3+}), Ulvöspinel (Ti)									
Ilm	91.7		86.2		85.9	87.5		84.2	
Gk/Mt	2.3	82.7	9.6	65.9	11.0	3.4	93.8	8.2	65.1
Hm/Ulv	6.0	17.3	4.2	34.1	3.1	9.1	6.2	7.6	34.9

The above compositions are some of those used in Figures 9 and 10. Numbers in parentheses indicate number of electron-microprobe analyses that were averaged. 1A & B: DG-1; very coarse magnetite with coarsely intergrown lamellar ilmenite. 2A,B,C: DG-3; coarse, granular intergrowth of magnetite and ilmenite, fully enclosed in partly serpentinized olivine. 3A & B: DG-6; small cube of magnetite with coarse ilmenite lamellae, on edge of silicate. 4A & B: 146-1176; very coarse ilmenite and magnetite with mutual grain-boundaries.

TABLE 3. COMPOSITION OF ILMENITE GRAINS OCCURRING ALONE

	#1 (2)	#2 (4)	#4 (4)	#5 (3)	#6 (4)	#7 (2)	#11 (2)
MgO	0.10	0.44	2.32	1.50	0.31	1.56	0.82
FeO	42.64	42.61	40.85	42.29	43.40	42.17	44.10
MnO	0.49	0.65	0.45	0.45	0.61	0.51	0.65
CaO	0.0	0.02	0.04	0.05	0.84	0.01	0.0
Al_2O_3	0.05	0.0	0.04	0.0	0.08	0.04	0.01
Cr_2O_3	0.03	0.0	0.16	0.10	0.06	0.04	0.08
Fe_2O_3	10.50	8.02	6.02	5.20	4.31	3.64	2.29
TiO_2	48.17	49.00	50.54	50.54	49.73	50.46	50.90
SiO_2	0.0	0.0	0.05	0.05	0.76	0.09	0.38
Total	101.98	100.74	100.47	100.18	100.10	98.52	99.23
Cation proportions, normalized to 3 oxygen atoms							
Mg	0.004	0.016	0.086	0.056	0.011	0.059	0.031
Fe^{2+}	0.887	0.894	0.846	0.883	0.911	0.895	0.933
Mn	0.010	0.014	0.010	0.010	0.013	0.011	0.014
Ca	0	0.001	0.002	0.001	0.023	0.001	0
Al	0.002	0	0.001	0	0.002	0.001	0
Cr	0	0	0.003	0.002	0.001	0.001	0.002
Fe^{3+}	0.195	0.151	0.112	0.098	0.081	0.069	0.044
Ti	0.901	0.924	0.941	0.949	0.939	0.962	0.967
Si	0	0	0.001	0.001	0.019	0.003	0.009
Total	1.99	2.00	2.00	2.00	2.00	2.00	2.00
Recalculated as Ilmenite (Fe^{2+}), Geikielite (Mg), Hematite (Fe^{3+})							
Ilm	90.1	90.0	85.6	89.4	94.6	90.5	94.6
Gk	0.4	1.7	8.7	5.6	1.2	6.0	3.2
Hm	9.9	7.7	5.7	5.0	4.2	3.5	2.2

Sample numbers correspond to those in Figure 12. Numbers in parentheses represent the number of electron-microprobe analyses that have been averaged. 1: DG-2; ilmenite with some minute clinopyroxene(?) inclusions; between orthopyroxene and plagioclase; 20μm beam. 2: DG-1; very coarse ilmenite intergrown with very coarse cubanite. 4: 146-1176; large grain of ilmenite with biotite on edges; at junction of plagioclase. 5: 146-1176; ilmenite intergrown with biotite and olivine; intercumulus to plagioclase. 6: DG-6; very small ilmenite rods in clinopyroxene. 7: 146-1093; small grain of ilmenite in serpentinized olivine. 11: 146-1093; small grain of ilmenite in serpentinized olivine, near secondary sulfides.

Some less common oxide textures also occur, for instance symplectic intergrowths of oxides and silicates (*cf.* Bonnichsen 1972b, Garrison & Taylor 1981). In one Inco sample, the composition of the magnetite in the symplectite closely matches that in the adjacent ilmenite–magnetite intergrowth, suggesting that the two oxide ocurrences were contemporaneous intercumulus precipitates or that they both re-equilibrated with the same late-stage fluids or melt.

COMPOSITION OF OXIDE MINERALS

Conditions of analysis

Three doubly polished thin sections from the Amax suite and six from the Inco suite were studied by wavelength-dispersion analysis with a fully automated JEOL-733 electron microprobe at Washington University. The standards are natural minerals and synthetic products of independently determined composition. "Spot analyses" were made with an electron beam focused to approximately 1 μm diameter; "broad-beam analyses" were made with a 20-μm beam. The operating conditions were 15 kV accelerating voltage and a current of 50 nA. Approximately 200 analyses were made of magnetite and ilmenite grains. The correction procedures are based on Bence & Albee (1968) and Albee & Ray (1970). The analyses were further recalculated to account for Fe^{3+} and Fe^{2+} (FERRIC program, Geophysical Laboratory) by assuming stoichiometry in the oxide phases.

For the purposes of geochemical comparison for geothermometry – oxygen barometry, the oxide assemblages are distinguished on the basis of whether ilmenite occurs alone or in ilmenite–magnetite intergrowths (Tables 2,3). Because of the rarity of magnetite, almost all the analyses of Amax samples are of ilmenite grains. Although ilmenite–magnetite intergrowths are common at Inco, there are also many isolated grains of ilmenite.

Combined gas chromatography – mass spectrometry (GC–MS) was performed on volatiles derived from six bulk samples by the MIDECO Company in Salt Lake City, Utah. Splits from the same samples were analyzed by two different techniques, each analysis reflecting (to a major degree) the compositions of fluid inclusions that decrepitated upon heating. In the headspace technique, a known weight of samples is heated at 400°C in a headspace vial for two hours. Then 0.5 cm^3 of headspace gas is withdrawn and injected into a gas-chromatographic column that is 1.5 metres long and contains 1% SP1000 on 60–80 mesh CarboPak B at 85°C. The detection-quantification system is a DuPont DP-102 GC/MS system. The mass range from 33 to 83 amu was scanned repeatedly at 50 amu per second. The carrier gas is helium flushed at 30 cm^3/minute.

The pyroprobe technique uses a Chemical Data Systems Model 120 Pyroprobe with a coiled platinum element that can be heated to controlled, reproducible temperatures in excess of 1200°C. A small quartz boat holds about 20 mg of sample, which is inserted into the pyroprobe and heated to decrepitate the fluid inclusions. The released gases are passed through the GC column described above. The separated gases that exit the column are detected by a mass spectrometer and a flame-ionization detector operating in tandem. The integrated peak-areas of selected species from the mass spectra can be compared to standard concentrations of gas. The amounts of the gases contained in the decrepitated fluid-inclusions can be calculated, providing semiquantitative analyses on the volatile contents of the rocks. In the present study, pyroprobe analyses were done at 700, 1000, and 1200°C. The 1000°C extractions are reported in Table 4. In both techniques, the complete operation is controlled by an H/P 21MXE computer system and associated software. These geochemical data on the volatiles included in the bulk-rock samples are regarded as semiquantitative and used for comparative purposes only, in conjunction with other geochemical techniques. The headspace technique is much closer to an equilibrium-extraction method than is the pyroprobe technique, in which the sample is heated (inhomogeneously) for only about one minute. The rock samples underwent no chemical pretreatment.

TABLE 4. COMPOSITION OF VOLATILES: GAS CHROMATOGRAPHY – MASS SPECTROMETRY

Sample	CH_4	C_2H_6	C_3H_8	CS_2	SO_2	COS	CO_2	H_2S
	Headspace technique; values in μg/g of sample*							
DG-1	ND	17.1	11.3	320.1	210.6	344.3	521	30.2
DG-2	6.4	62.3	32.0	462.3	39.8	574.3	951	57.3
DG-6	19.8	ND	ND	334.4	9.8	255.3	651	15.1
146-1093	53.4	285.0	317.1	652.1	3.6	396.1	1321	208.5
146-1176	13.1	110.2	216.2	393.9	ND	359.0	1060	105.0
146-1346	ND	46.4	92.6	210.3	ND	80.4	890	ND
	Pyroprobe extraction at 1000°C; values in μg**							
DG-1	0.24	0.03	ND	ND	46.7	NA	51.7	4.2
DG-2	1.0	0.03	ND	0.15	19.2	0.014	41.6	3.9
DG-6	0.014	TR	ND	0.13	9.03	0.004	91.9	4.1
146-1093	0.49	0.03	ND	0.18	1.17	TR	75.6	16.3
146-1176	0.044	0.008	ND	0.17	4.13	0.016	45.8	18.4
146-1346	0.43	0.018	ND	0.002	0.29	TR	39.2	2.1

* Accuracy approximately ± 5% relative. ** Semi-quantitative values; useful for comparisons. D.N. Osborne, analyst, MIDECO. NA not analyzed; TR trace

Compositions of the oxide phases

The major solid-solution affecting ilmenite involves Fe^{3+} (hematite component) and Mg (geikielite component). In ilmenite from both suites, MgO ranges up to 2.32 wt.%. Ferric iron contents range from about 2.29 to 8.02 wt.% Fe_2O_3 in isolated ilmenite grains, *i.e.*, 2.2 to 7.7. mole % hematite in the three-component system ilmenite–hematite–geikielite (Table 3). In the ilmenite–magnetite intergrowths, ilmenite generally contains between 3 and 9 mole % hematite, although one sample (also very Al-rich) has 23.1 mole % hematite (Table 2). These values are similar to those reported by Hardyman (1969) for ilmenite occurring in the South Kawishiwi complex (0.6–3.9 wt. % MgO, 0.8–6.4 wt.% Fe_2O_3). Hardyman (1969) did not provide compositions of the magnetite that also occurs in his suite.

In general, the isolated grains of ilmenite from Amax have a lower Fe^{3+} content and a higher Mg content than from Inco. At Inco, the ilmenite in the magnetite–ilmenite intergrowths tends to have higher Fe^{3+} and lower Mg than do isolated grains in the same suite. The contrast in Mg contents probably in part reflects partitioning between ilmenite and magnetite, although the magnetite is also low in Mg (usually <0.5 wt.% MgO). The Mg content is also controlled by partitioning with silicates such as olivine and pyroxene. Hardyman (1969) reported, however, that the correlation between Mg content of coexisting olivine and ilmenite is poor.

The major contaminants in the magnetite grains are Cr (up to 15.37, but usually <2 wt.% Cr_2O_3) and Al (up to 6.46, but usually <2 wt.% Al_2O_3). Several spot-analyses and at least one broad-beam analysis were done on most of the magnetite grains that were studied. Although the grains are not compositionally zoned in the classic sense, there are considerable variations among the results of spot analyses. These are due to abundant, minute (exsolution) lamellae of spinel, many of which are visible in reflected light and with compositional scans on the scanning-electron microscope (SEM). Variations in Al content of the magnetite probably reflect the presence of spinel lamellae. The infrequent occurrence of high-Cr magnetite suggests that there also may be some remnants of an earlier episode of magnetite precipitation or perhaps some xenocrysts among the oxide grains.

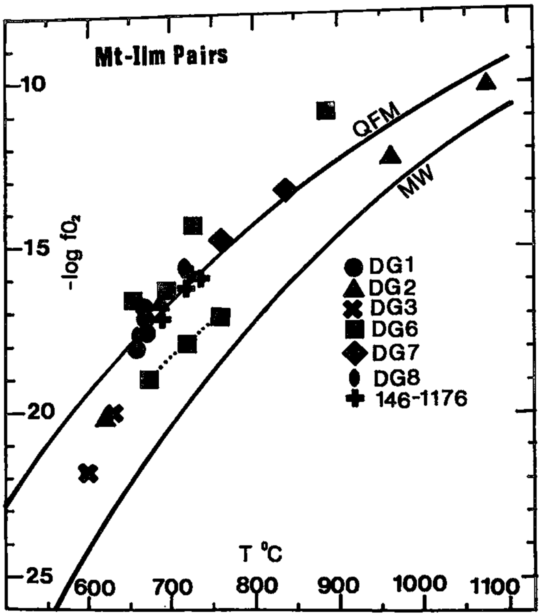

FIG. 9. T-$f(O_2)$ conditions inferred from the compositions of coexisting Fe–Ti-oxide grains. Calculated according to Lindsley & Spencer (1982). QFM (Chou 1978) and WM (Eugster & Wones 1982) oxygen-buffer curves at 1.5 kbar are plotted for reference. See text for further explanation.

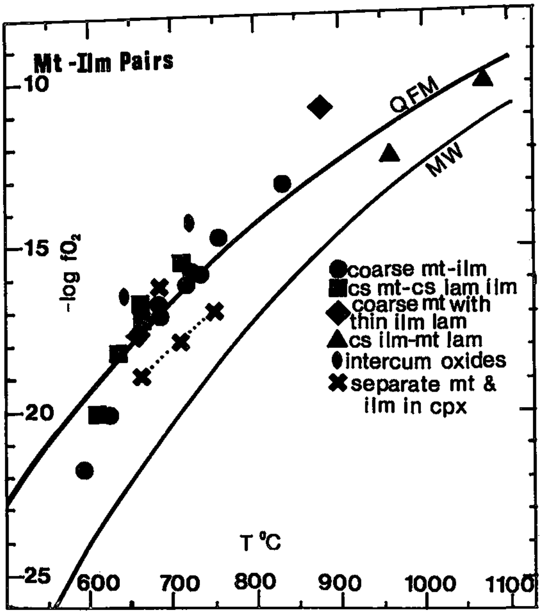

FIG. 10. Same data set and calculations as in Figure 9. Data plotted according to textural types listed in symbol key. See text for further explanation.

The average of several spot-determinations usually is very similar to the broad-beam determination. These presumed estimates of bulk composition of magnetite (excluding any visible lamellae of ilmenite) are used in the T-$f(O_2)$ calculations described in a following section.

Compositions of included volatiles

Combined gas chromatography - mass spectrometry was performed on crushed sieved samples (smaller than 70 mesh) of DG-1, DG-2, DG-6 from the Inco suite, and 146–1093, 146-1176 and 146–1346 (hornfels zone) from the Amax suite. Several generalizations can be made about the data in Table 4. Both analytical methods show that CO_2 is the dominant species and that the more oxidized sulfur species SO_2 is more abundant than H_2S in the Inco samples. Even though H_2S usually is subordinate, it is much more abundant in most of the Amax than in the Inco rocks. In the headspace analyses, the Amax samples show much greater abundance of hydrocarbon species than those from Inco.

The three Amax samples are known to be quite different mineralogically: sample 146–1093 is typical of Amax; 146–1176 is the only Amax sample with both magnetite and ilmenite, and 146–1346 is from the hornfels zone and obviously contains large xenoliths. In both sets of GC–MS results, the values for 146–1176 resemble those from 146–1093 much more than those from the Inco suite. In contrast, the gas composition from the 146–1346 hornfels are distinctly different from those in any other sample. Therefore, the semiquantitative extractions of gas appear to confirm the mineralogical data concerning the relatively more oxidized nature of the Inco compared to the Minnamax suite.

GEOTHERMOMETRY – OXYGEN BAROMETRY

Assumptions

The thermodynamic basis and experimental calibration of the Fe-Ti-oxide geothermometer – oxygen barometer have been used by petrologists for many years (*e.g.*, Buddington & Lindsley 1964, Lindsley 1976, Powell & Powell 1977). The approach is based on the fact that the coexistence of specific compositions of ilmenite-hematite$_{ss}$ and ulvöspinel-magnetite$_{ss}$ buffers the fugacity of oxygen in the system Fe–Ti–O. Furthermore, in complex natural systems controlled by other $f(O_2)$-buffering mechanisms, the Fe–Ti-oxides mutually adjust their composition to reflect the prevailing T-$f(O_2)$ conditions.

The two pertinent equations are (Powell & Powell 1977):

$$\begin{array}{ccccccccc} FeTiO_3 & + & Fe_3O_4 & = & Fe_2O_3 & + & Fe_2TiO_4 & (1) \\ \text{ilmenite} & & \text{magnetite} & & \text{hematite} & & \text{ulvöspinel} & \\ Ilm_{ss} & + & Mt_{ss} & = & Ilm_{ss} & + & Mt_{ss} & \end{array}$$

which is temperature-dependent, and

$$6\,Fe_2TiO_4 + O_2 = 6\,FeTiO_3 + 2\,Fe_3O_4 \quad (2)$$

which is $f(O_2)$-dependent.

Several criteria must be met in order to make reasonable thermobarometric interpretations. A unique temperature and $f(O_2)$ can be calculated only if a constant pressure is assumed and if both oxide phases are present and in equilibrium (constraints of the phase rule). The calculated T-$f(O_2)$ solutions represent the last episode of re-equilibration of the oxides. In gabbroic rocks like those in the Duluth Complex, the calculated temperatures characteristically are much below the liquidus. The re-equilibration typically produces bodies of ilmenite "exsolved" from titaniferous magnetite during cooling and oxidation (*e.g.*, Buddington & Lindsley 1964, Haggerty 1976).

In the present study, the Fe–Ti oxides admittedly do not record their original high-temperature igneous conditions. As seen in Figures 9 and 10, however, they appear to have recorded various steps in the cooling path of the intrusive bodies. This is significant for at least two reasons. Firstly, criteria are needed to distinguish the conditions of crystallization, including $f(O_2)$, of the several mafic and ultramafic bodies in the Duluth Complex. Secondly, Cu-Fe-sulfides are observed to have selectively replaced magnetite in re-equilibrated magnetite–ilmenite intergrowths (Fig. 11; Pasteris 1984). This means that sulfides were still forming during or after the T-$f(O_2)$ episodes recorded by the oxides. These data will increase our understanding of sulfide segregation and precipitation at Duluth.

Careful documentation was made of the different textural types of oxides so that T-$f(O_2)$ distinctions could be made among grains that were formed or equilibrated under different conditions. Complex intergrowths potentially contain much information. Where coarse magnetite and ilmenite coexist, and the magnetite$_{ss}$ in turn has small domains of ilmenite$_{ss}$ in it, two episodes of oxidation–exsolution are apparent. Broad-beam analysis of the *bulk* composition of the coarse magnetite (with its lamellae) and ilmenite provides one T-$f(O_2)$ datum, whereas spot analysis of the magnetite host and its fine lamellar inclusions of ilmenite should provide a lower T-$f(O_2)$ datum (*cf.* Bowles 1977).

Methods of calculation

As seen in equations 1 and 2, the compositions of the coexisting oxide phases must be stated in terms of mole percentages of the four end-members. If only Fe, Ti and O comprise the phases, this calculation is trivial, and one then proceeds to a mathematical (*e.g.*, Powell & Powell 1977, Spencer & Lindsley 1981) or graphical (*e.g.*, Spencer & Lindsley 1981) solution to obtain temperature and oxygen fugacity. The Duluth oxides, however, also contain non-negligible amounts of Mg, Mn, Cr and Al (Tables 2, 3). The thermodynamic handling of such contaminants in the formulation of this geothermobarometer has been debated for many years (*e.g.*, Powell & Powell 1977, Spencer & Lindsley 1981). Two of the most recent formulations are the empirical approach of Lindsley & Spencer (1982) and the theoretical approach of Stormer (1982).

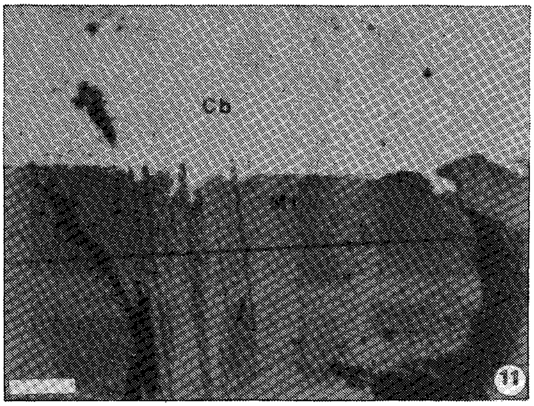

FIG. 11. Cubanite (Cb) replacing the magnetite portion of a magnetite-ilmenite (Mt; ilm) intergrowth. Mobility of Cu and subsequent precipitation of cubanite post-date the re-equilibration of the Fe- Ti oxides and their development of intergrowths. DG-8, Inco. Scale bar 30 μm. Reflected light, oil immersion.

Both of the above methods of calculation were used on the present data. The T-$f(O_2)$ pairs calculated by each method are very similar to each other, usually within 20°C and 0.5 log $f(O_2)$ units. This compares favorably with the estimated uncertainties of Spencer & Lindsley (1981) [40–80°C and 0.5–1.0 log units $f(O_2)$ ($2\ \sigma$)] for their model of the pure Fe-Ti-O system. The greater the content of minor elements in the oxides, the greater are the T-$f(O_2)$ differences between the two formulations.

The points actually plotted in Figures 9 and 10 were derived by calculating equivalent end-member oxides by the method of Lindsley & Spencer (1982), and then plotting the oxide pairs on the 1 atm T-$f(O_2)$ calibration curves of Spencer & Lindsley (1981). For reference, the QFM and WM buffer curves for quartz–fayalite–magnetite (Chou 1978) and wüstite-magnetite (Eugster & Wones 1962) are plotted for a total pressure of 1.5 kbar (making assumptions about the probable depth of intrusion of the Duluth Complex). The solid-phase curves of

Spencer & Lindsley (1981) at 1 bar would be elevated slightly on the diagram for 1.5 kbar pressure. However, it is not the specific values that are significant, but rather the general trends.

T-*f*(O_2) *plots*

In Figure 9, the data for coexisting ilmenite and magnetite pairs are distinguished according to sample location. As indicated in Tables 2 and 3, each point on the graph represents several determinations. Figure 10 is a plot of the same data, but here the symbols designate different textural types of coexisting ilmenite and magnetite. Three different types of variations can be evaluated: 1) overall T-$f(O_2)$ trends, 2) differences among individual rock-samples, and 3) differences among textural types.

Figure 9 shows that there is a wide range of conditions of equilibration. Most points lie between 850° and 650°C, and within 1 log $f(O_2)$ unit of the QFM buffer at $P_{total} = 1.5$ kbar. No points indicate more reducing conditions than approximately half-way between the QFM and WM buffers. Only one Minnamax sample, 146–1176, appears on the plot, because it is the only specimen investigated that contains coexisting ilmenite and magnetite. The data for 146–1176, which has very coarse intergrowths, lie almost exactly on the QFM curve.

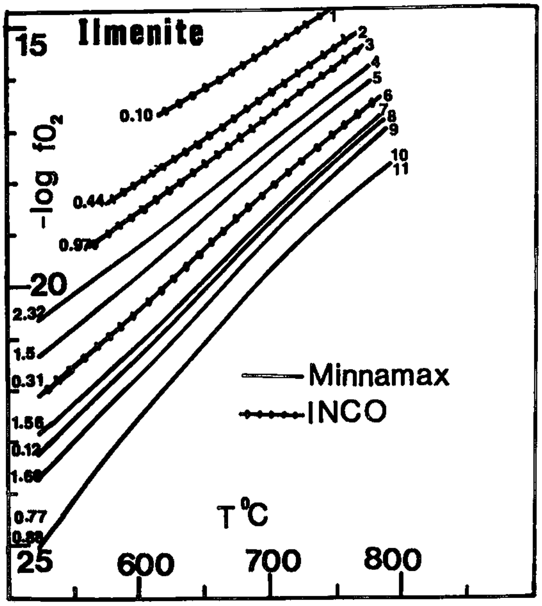

FIG. 12. Inferred T-$f(O_2)$ conditions of ilmenite grains occurring isolated from magnetite. The curves are ilmenite–hematite isopleths taken from Spencer & Lindsley (1981). Ilmenite compositions calculated according to Lindsley & Spencer (1982). Numbers at left of isopleths represent wt.% MgO in ilmenite. Samples are: 1 DG-2, 2 DG-1 (coarse ilmenite intergrown with coarse cubanite), 3 DG-2 (coarse ilmenite intergrown with coarse cubanite), 4 and 5 146–1176, 6 DG-6 (small rods of ilmenite enclosed in augite), 7, 9 and 11 146-1093, 8 and 10 146–1346 (hornfels zone).

Within individual samples, there are wide ranges in conditions of equilibration. Few other generalizations can be made except that the data from samples 146–1176, DG1, and DG8 cluster very closely around the QFM curve.

An interpretation of the data as a function of the textural type (Fig. 10) was undertaken for comparison with Oliver's (1978) work on ilmenite–magnetite intergrowths in granulite- and amphibole-facies gneisses. He found that the fine-grained intergrowths of oxides indicate temperatures of about 1000°C, whereas coarse intergrowths indicate only 500°C. In addition, the lower-temperature oxides recorded values of $f(O_2)$ above QFM, in contrast to the high-temperature ones. Oliver (1978) concluded that as the metamorphic rocks cooled, they were buffered at about Ni-NiO conditions.

The six textural types that were distinguished in the oxide phases from Duluth (Fig. 10) are: 1) coarse magnetite and coarse ilmenite, which are usually granular (presumed oxidation-exsolution with subsequent recrystallization), 2) coarse magnetite with *wide* ilmenite lamellae (probably advanced oxidation-exsolution), 3) coarse magnetite with *thin* ilmenite lamellae (probably early stage of oxidation-exsolution), 4) coarse ilmenite with magnetite lamellae (primary ilmenite and rare products of reduction–exsolution) 5) small oxide grains (intercumulus or cumulus), and 6) separate magnetite and ilmenite bodies in clinopyroxene (possibly exsolution from a high-temperature pyroxene).

Again, few patterns are clear. The separate, small grains of magnetite and ilmenite in augite produce a T-$f(O_2)$ trajectory that consistently lies about 1 log $f(O_2)$ unit below QFM. These isolated, silicate-mantled oxide grains may reflect the true ambient $f(O_2)$ during their crystallization. The small grains of intercumulus oxides appear more oxidized than most other textural types. The coarsest intergrowths of magnetite and ilmenite appear to be products of extensive oxidation-exsolution, diffusion and recrystallization, with final equilibrium between 850°C and 600°C. The T-$f(O_2)$ trajectory for these intergrowths lies above QFM at higher temperatures and becomes more reducing than QFM at lower temperatures, *i.e.*, it approximately follows an ulvöspinel isopleth.

Figure 12 is a plot of ilmenite isopleths for individually occurring grains of ilmenite in the Inco and Minnamax suites. The curves are taken from Spencer & Lindsley (1981). As discussed above, the presence of only one Fe–Ti-oxide phase does not define a specific T-$f(O_2)$ point for a given pressure (here plotted at 1 bar). An ilmenite isopleth is a univariant curve that shows the *minimum* $f(O_2)$ at a given temperature. The portion of the curve between 550°C and 850°C is drawn here because of the assumed temperatures of equilibration. As discussed below, this is a less reliable means of evaluating $f(O_2)$ differences. The assumptions are that the more Fe^{3+}-rich ilmenite represents a higher value of $f(O_2)$ than the lower-Fe^{3+} grains, and that these are equilibrium compositions of ilmenite. This permits estimation of the $f(O_2)$ differences between two samples at a chosen temperature. Again, only broad trends are being evaluated.

Because ilmenite alone gives only a minimum value for $f(O_2)$, however, the values *could* be the same for both suites of rocks. For instance, the lack of magnetite could indicate a lower a_{FeO}/a_{TiO_2} in the Amax compared to the Inco suite. Examination of other heterogeneous equilibria in the rocks may indicate whether the proposed Fe^{3+} - $f(O_2)$ relationship holds (D. Lindsley, pers. comm.). Consider the following:

$$\underset{\text{Ol}}{2\ Fe_2SiO_4} + O_2 = \underset{\text{ilm}}{2\ Fe_2O_3} + \underset{\text{liq}}{2\ SiO_2} \qquad (3a)$$

$$K = \frac{\left(a^{ilm}_{hm}\right)^2 \left(a^{liq}_{SiO_2}\right)^2}{\left(a^{ol}_{fa}\right)^2 \left(f(O_2)\right)} \qquad (3b)$$

The coexistence of pyroxene and olivine in these suites fixes the activity of SiO_2. Assuming that the oxide and silicate grains are in equilibrium, one can test several possibilities. If the $f(O_2)$ is actually the same in both suites, then the assemblage with the larger a^{ol}_{fa} also must have the larger a^{ilm}_{hm}. The latter ilmenite–olivine compositional relationship is not true here (olivine data: Pasteris 1984). If the earlier hypothesis instead is true, *i.e.*, that a larger a^{ilm}_{hm} reflects a larger $f(O_2)$, then the larger a^{ilm}_{hm} must be accompanied by a smaller a^{ol}_{fa}. This is indeed the compositional relationship here. Therefore, the smaller a^{ilm}_{hm} in the lone ilmenite from Amax compared to those from Inco may reflect relatively more reducing conditions at Amax. In further support of this relationship is the presence of troilite (more reduced) and vapor-precipitated graphite at Minnamax, but most commonly only hexagonal pyrrhotite (more oxidized) at Inco (Pasteris 1984). In addition, in the Water Hen intrusive body to the south (see Fig. 1), there appears to be a direct relationship between the coexistence of graphite and ilmenite with the absence of magnetite (W. Ulland, American Shield, 1984, pers. comm.).

Based on the assumption of a direct relationship between $f(O_2)$ and Fe^{3+}, several patterns can be recognized in Figure 12. As expected, the Inco samples consistently lie at higher $f(O_2)$ values than most of the Minnamax samples. The only samples of Minnamax ilmenite that represent $f(O_2)$ values near those from Inco come from sample 146–1176 (which elsewhere contains magnetite). The MgO contents of ilmenite (listed to the left of the isopleths, in weight %) do not correlate with the Fe^{3+} contents, which may reflect low-temperature re-equilibration with the ferromagnesian silicates (D. Lindsley, pers. comm.). Two other features of ilmenite are consistent with the corresponding ilm–mt data. Isopleths 2 and 3 represent coarse ilmenite intergrown with coarse (>3 mm) cubanite. Isopleth 6 represents small rods of ilmenite in clinopyroxene. Just as in the ilm–mt data, it appears that early phenocrysts and exsolution products within silicates lie at a lower $f(O_2)$ than later (re-equilibrated?) intercumulus phases. The internal consistency of the ilm–mt and ilmenite-alone data supports the usefulness of this approach (Fig. 12).

INTERPRETATION OF THE T-fO_2) DATA

Justification

Previous studies have shown that the Fe–Ti-oxide geothermobarometer gives reliable T-fO_2) values of the conditions of original formation only where the rocks are rapidly quenched. In re-equilibrated intrusive rocks, one can theoretically retrieve the original T-fO_2) data by reconstructing the compositions of the primary phases from the present intergrowths. In such calculations one must assume, however, that the individual coexisting oxides have undergone only *internal* re-equilibration, but not external cation exchange (Hammond & Taylor 1982). Only in one case were the Duluth oxides amenable to this approach owing to the fine grain-size of the second-generation intergrowths. Lindsley's (1976) petrological studies and the experiments of Hammond & Taylor (1982) show that during cooling of an oxide-bearing system, titanomagnetite usually re-equilibrates (oxidizes) more readily than the ilmenite becomes reduced. This accounts for the rarity of magnetite lamellae in ilmenite at Duluth and elsewhere. Some of the ilmenite compositions depicted in Figure 12 may have persisted metastably at temperatures and oxygen fugacities where magnetite should coexist with ilmenite. It thus appears that the ilmenite more readily preserves its high-temperature conditions than does titanomagnetite.

Hammond & Taylor (1982) found that the rate-controlling factor in the (synthetic) re-equilibration of both oxide phases is the flow rate of reactant gas. There is evidence for a late-stage, mobile fluid in the Duluth troctolites (*e.g.*, Pasteris 1984). Therefore, intercumulus oxides exposed to a circulating fluid phase probably re-equilibrated more readily than oxides fully enclosed in silicate grains.

Inferences from oxide and sulfide equilibria

Both the mt–ilm and ilmenite-alone data suggest the following sequence. Early cumulate oxides and grains that exsolved early from high-temperature silicates were more reduced than the QFM buffer. The coarse ilmenite intergrown with coarse cubanite (Fig. 3) and the intercumulus, re-equilibrated intergrowths of mt–ilm (Fig. 6) record $fO_2)$ values at or above QFM, which may be associated with later, more oxidizing conditions. As the entire system of cumulus and intercumulus rocks cooled, it approached an intermediate $fO_2)$, as is shown in the cooling trajectory for the well-equilibrated, coarse mt–ilm intergrowths on Figure 10 (filled circles).

ASSIMILATION MODEL

The $fO_2)$ trends reported above are of special significance if the oxides and sulfides were in equilibrium during their formation and re-equilibration. Equilibrium is assumed because of the consistently more oxidized sulfides and oxides at Inco and the consistently more reduced assemblage at Minnamax. Furthermore, there are smooth mutual grain-boundaries between sulfides and coarsely exsolved oxides, and late Cu–Fe sulfides selectively replace portions of finely exsolved Fe–Ti oxides (Fig. 11).

The compositional data on coexisting oxide and sulfide phases can be used to evaluate the range of

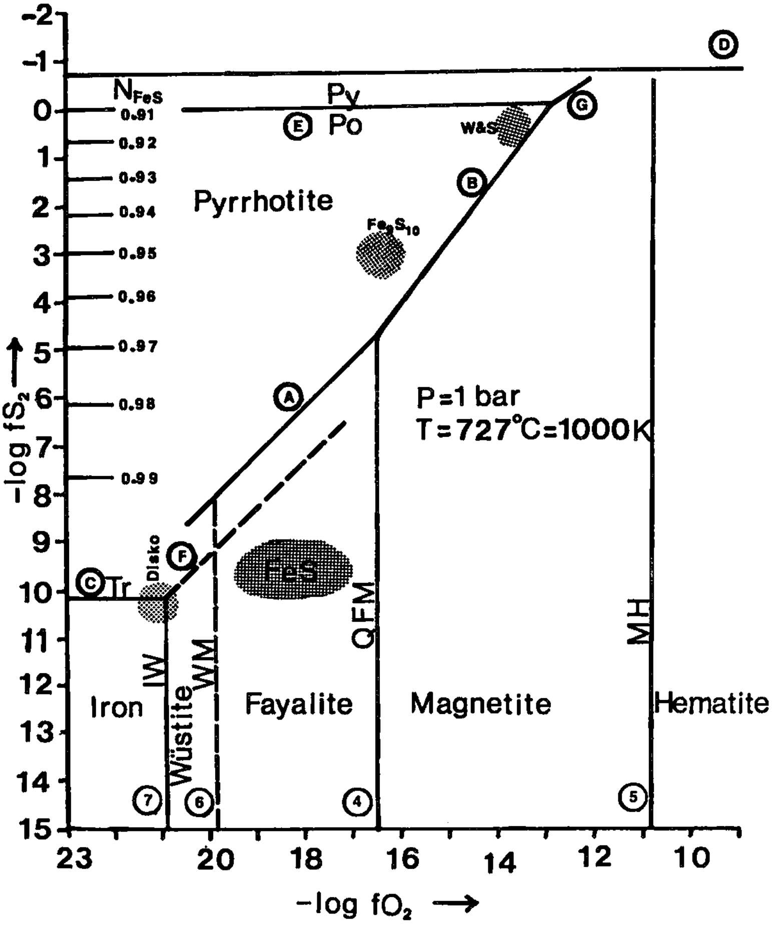

FIG. 13. An $f(O_2)$ - $f(S_2)$ plot at 727°C and 1 bar showing the inferred conditions of re-equilibration of the Inco suite (area marked Fe_9S_{10}) and Minnamax suite (FeS). The $f(O_2)$ - $f(S_2)$ conditions of two other contaminated melts are shown for comparison: calc-alkaline tuffs (W & S) of Whitney & Stormer (1983) and iron-bearing basaltic glass (Disko) of Pedersen (1979a, b). See text for further explanation and a listing of the reactions considered. Diagram after Whitney & Stormer (1983).

fO_2) and fS_2) values in the rocks during their re-equilibration. Temperature-fO_2) data are available from the Fe–Ti oxides, and the specific composition of the coexisting pyrrhotite phase defines an fS_2) for the same temperature (Toulmin & Barton 1964). The point 727°C (1000 K) and log fO_2) ~ -16.0 was chosen from Figure 9 as representative of the re-equilibration conditions at Inco. For the coexisting hexagonal pyrrhotite Fe_9S_{10}, that implies log fS_2) ~ -2.97. At the same temperature, the isolated grains of ilmenite at Minnamax show a wide range in fO_2). For ilmenite 7 (Fig. 12) coexisting with troilite, for instance, the conditions at 727°C are log fO_2) ~ -18.5 and log fS_2) ~ -10.1. Many of the iron sulfide grains at Minnamax actually consist of troilite that contains lamellae of hexagonal pyrrhotite. Thus, log fS_2) actually was greater than -10.1, and log fO_2) ranged from about -17.2 to -19.5.

The inferred conditions of fugacity for the Duluth minerals are plotted on Figure 13, in relation to the stability fields of several phases of interest. The lines on the diagram represent the following reactions:

$$2Fe_3O_4 + 3SiO_2 = 3Fe_2SiO_4 + O_2 \tag{4}$$

$$6Fe_2O_3 = 4Fe_3O_4 + O_2 \tag{5}$$

$$2Fe_3O_4 = 6FeO + O_2 \tag{6}$$

$$2FeO = 2Fe + O_2 \tag{7}$$

$$Fe_2SiO_4 + S_2 = 2FeS + SiO_2 + O_2 \tag{A}$$

$$Fe_3O_4 + \tfrac{3}{2}S_2 = 3FeS + 2O_2 \tag{B}$$

$$Fe + \tfrac{1}{2}S_2 = FeS \tag{C}$$

$$S_2\ (gas) = 2S\ (liquid) \tag{D}$$

$$FeS + \tfrac{1}{2}S_2 = FeS_2 \tag{E}$$

$$2FeO + S_2 = 2FeS + O_2 \tag{F}$$

$$Fe_3O_4 + 3S_2 = 3FeS_2 + 2O_2 \tag{G}$$

Although pyrite is not stable above about 743°C at one bar and none was identified at Duluth, the pyrite–pyrrhotite boundary is shown for reference. At the chosen temperature of 727°C, the Py–Po reaction has almost the same $f(S_2)$ as the sulfur-condensation curve. The N_{FeS} of the pyrrhotite in equilibrium with pyrite is about 0.91 (Barton & Skinner 1979).

All the reaction lines were calculated from data in Robie *et al.* (1978), except reactions (D) and (E), based on the data of Barton & Skinner (1979). For most of the lettered reaction-curves, thermodynamic data for troilite were used. The dashed isopleths for pyrrhotite (N_{FeS} is equivalent to twice the atomic % Fe in pyrrhotite) are calculated according to Toulmin & Barton (1964).

As noted in the introduction of this paper, assimilation was an important process in the development of the sulfide ores at Duluth. Ideally, one would like to trace the T-$f(O_2)$-$f(S_2)$ path of the parent melt of the troctolite as it reacted with the country rocks, distilled volatiles and absorbed other components from it, and eventually cooled and precipitated silicate, oxide and sulfide phases.

Whitney & Stormer (1983) have done such an analysis for the calcalkaline magma that produced the Fish Canyon Tuff in the San Juan Mountains volcanic field. The T-$f(O_2)$-$f(S_2)$ regime for their re-equilibrated samples is also shown on Figure 13 (they actually did their calculations for 800°C = 1073 K). Whitney & Stormer (1983) considered the assimilation of crustal material that had original pyrite and magnetite, which, when heated and reacted, yielded pyrrhotite and oxygen. As the temperature of the assimilated material increased, the $f(O_2)$ and $f(S_2)$ of the system rose rapidly along the reaction curve. As seen in Figure 13, the values eventually approached the sulfur-condensation curve (see also Whitney 1984).

Similar processes probably occurred at Duluth when portions of the adjacent pyrite- and magnetite-bearing Virginia Formation were assimilated. The presence of abundant graphite in these sediments, however, prevented the $f(O_2)$ of the system from rising greatly, perhaps not appreciably above the QFM buffer. This hypothesis is supported by the data on the Fe–Ti oxides. The geological relations in the Duluth Complex (Weiblen & Morey 1980) suggest that the Inco body was less contaminated by graphitic sediments than the Minnamax body, which may explain why the Minnamax assemblages are consistently more reduced.

For comparison, the $f(O_2)$-$f(S_2)$ conditions in the troilite- and native-iron-bearing basaltic glasses in Disko, Greenland (Pedersen 1979a, b) are plotted in Figure 13 (assuming same oxygen and sulfur buffers at 727°C as at their quench temperature of 1200°C). Graphite-bearing shales reacted with the intruding dykes at Disko to produce locally very reducing conditions that stabilized even native iron.

Work done by Haughton *et al.* (1974), Shima & Naldrett (1975), Buchanan & Nolan (1979), among others, has shown the complex dependence of sulfide immiscibility on T, $f(O_2)$, $f(S_2)$, and bulk composition of the melt, specifically for mafic magmas. For coexisting sulfide and silicate melts, (1) the higher the $f(O_2)$, the higher the sulfur concentration required in the silicate melt to maintain an immiscible sulfide liquid at constant $f(S_2)$, whereas (2) the higher the $f(S_2)$, the lower the sulfur concentration required in the melt to maintain an immiscible sulfide liquid at constant $f(O_2)$ (Haughton *et al.* 1974, Buchanan & Nolan 1979).

Knowledge of the $f(O_2)$-$f(S_2)$ history of the Duluth melts is therefore necessary in order to infer when and how sulfide immiscibility occurred. Many of the existing experimental data pertain to melts studied at 1200°C, *i.e.,* they are appropriate to sulfide immiscibility that occurs very early during crystallization. These experiments are not so relevant for cases of assimilation; in fact, at Duluth the textural evidence suggests that sulfide immiscibility occurred late in the sequence of crystallization.

However, by making some assumptions we can extrapolate from the conditions at 727°C as shown in Figure 13 to the possible conditions near 1200°C. In the chemically open system at Duluth, it is not possible to pinpoint the exact compositions of the oxide and sulfide phases at 1200°C. The intergrowth textures observed give some indication of subsequent re-equilibration. The purpose of the following exercise is to make some reasonable assumptions to allow us to evaluate some of the models for Duluth-type sulfide deposits.

From the evidence above, assume that the QFM buffer represents the highest $f(O_2)$ obtained by the Duluth melts. If this is correct, the $f(S_2)$ needed to cause sulfide saturation can be calculated. In addition, if the bulk composition of the pyrrhotite phases has not changed greatly, one may calculate the $f(S_2)$ necessary at elevated temperatures to stabilize the most sulfur-rich pyrrhotite at Duluth, again indicating the $f(S_2)$ required.

These calculated conditions can be compared with the data of Buchanan & Nolan (1979) for sulfide saturation at 1200°C in melts equivalent to Bushveld diorites. The maximum thermal stability of "pyrrhotite" is about 1190°C (Craig & Scott 1974); this temperature, chosen for the following calculations, is higher than for any of the calibration experiments on pyrrhotite by Toulmin & Barton (1964), but permits comparison with the silicate-melt data. Log $f(O_2)$ is approximately -8.4 for the QFM buffer, and log $f(S_2)$ is approximately +0.7 for pyrrhotite of composition $N_{FeS} = 0.95$.

For their Bushveld-type melts (~16 wt.% FeO) held along the QFM buffer at 1200°C, Buchanan & Nolan found that log $f(S_2)$ must be at least -1.0 to cause sulfide immiscibility. The bulk rocks at Inco have about 10 wt.% total FeO (Weiblen & Morey 1980). This means that log $f(S_2)$ must be ~0.5 units higher, but that less dissolved sulfur is actually needed to induce immiscibility in this silicate melt than in one with a higher FeO content (Haughton *et al.* 1974, Buchanan & Nolan 1979)

This is already a relatively high fugacity of sulfur. To stabilize pyrrhotite of composition $N_{FeS} = 0.95$ would require almost 2 orders of magnitude higher $f(S_2)$. The above can be interpreted, for instance, to suggest (1) that this is why sulfide immiscibility did not occur very early during crystallization (before assimilation), or (2) that the melt actually was in its more reduced state when immiscibility occurred [lower $f(S_2)$ required for more reduced melts].

This emphasizes the importance to sulfide melt segregation of keeping the $f(O_2)$ moderate. Thus, it may be very significant for sulfide ores in major igneous bodies that not only assimilation of sulfur occur (*e.g.,* Buchanan & Nolan 1979), but also that reducing materials be assimilated, in order that very high fugacities of sulfur not be required for saturation.

SUMMARY AND CONCLUSIONS

Textural similarities in the troctolites from the Inco and Minnamax suites suggest that the timing of the precipitation of sulfide, oxide, and silicate phases was approximately the same in both intrusive bodies. There are, however, consistent differences in the $f(O_2)$ and $f(S_2)$ values of the two assemblages. An environment of higher $f(O_2)$ and $f(S_2)$ prevailed at Inco, as indicated by the presence of magnetite in addition to ilmenite, a relatively high Fe^{3+} content in isolated grains of ilmenite, and the dominance of hexagonal pyrrhotite over troilite. The Minnamax suite represents lower $f(O_2)$ and $f(S_2)$ conditions, as shown by the virtual absence of magnetite, lower values of Fe^{3+} in ilmenite, and the abundance of troilite. Combined GC–MS analysis of trapped volatiles in bulk-rock samples also confirms the above $f(O_2)$ relationships.

Ishihara (1981) has subdivided igneous rocks (particularly felsic to intermediate calcalkaline rocks) into ilmenite-bearing and magnetite-bearing series. He documented the chemical and mineralogical differences between the two groups and attempted to relate these to the differences in the ore deposits that commonly occur in each suite. Ishihara concluded that the consistently lower $f(O_2)$ of the ilmenite-series rocks is due to contamination by reducing crustal material. Such an assimilation model is appropriate at Duluth, because crustal foundering would have been a major part of the incipient rifting that probably accompanied the intrusion of the Complex. It is significant, however, that "ilmenite-series and magnetite-series gabbros" occur in such close proximity. The lower fugacities in the southern troctolite may be due to the more effective assimilation of graphitic sediments at Minnamax than at Inco.

It is evident, especially from the magnetite-ilmenite intergrowths in the Inco suite, that the oxide phases have undergone extensive re-equilibration during cooling, a common occurrence in slowly cooled gabbroic bodies. Consideration of the different textural occurrences of the oxides suggests that very early precipitates, which were chemically isolated within silicate grains, formed under $f(O_2)$ conditions slightly below the QFM buffer. The early oxides may record the cooling of a rock-dominated system along an oxygen buffer below QFM. The later, intercumulus oxides indicate $f(O_2)$ values at or slightly above QFM, suggesting that later fluids were more oxidizing. Upon cooling, these intercumulus oxides appear to have followed a T-$f(O_2)$ trajectory that became somewhat more reducing than QFM. This could be due to equilibration with the earlier phenocrysts or to the later influx of more reducing components, as described in the assimilation model.

The primary T-$f(O_2)$ relations can be accounted for by a model in which pyrite and magnetite reacted during the heating of assimilated crust and caused $f(O_2)$ and $f(S_2)$ to rise relative to the rock buffers. The elevation in oxygen fugacity was constrained to about the QFM buffer owing to the accompanying presence of graphite in these sediments.

Assimilation provided an important source of sulfur for the abundant Cu–Fe–Ni sulfides at Duluth. The assimilation of carbon was also essential to the development of the ore deposits, because it moderated the $f(O_2)$ level in the melt and thus aided in the development of an immiscible sulfide liquid.

Whitney & Stormer (1983) considered assimilation processes in melts of much less mafic composition than the Duluth troctolites or Bushveld diorites. However, it may be significant that abundant sulfide immiscibility does not occur in rocks of intermediate composition. If such melts are generated by assimilation of relatively oxidizing crust, then the ensuing rise in $f(O_2)$ relative to a typical buffer (Whitney & Stormer 1983) may prevent sulfide immiscibility. Instead, dissolved sulfur may increase in concentration in the melt, become enriched in late-stage fluids, and eventually produce the hydrothermal sulfide deposits common to intermediate rocks rather than immiscible sulfide segregations. Of course, there are numerous other important differences between the two rock types and their environments of genesis.

Similarly, at Duluth one could infer that the obvious mobility of Cu–Fe sulfides during the later, more oxidizing episode recorded by the Fe–Ti oxides was due to the presence of some type of hydrothermal solution. In sample 146–1176, the only Minnamax sample that was sufficiently oxidizing to contain magnetite, very extensive replacement by Cu–Fe-sulfides has occurred. Almost no pyrrhotite remains in the thin section, and large grains of homogeneous cubanite are present, rather than the cubanite–chalcopyrite intergrowths that are expected from the re-equilibration of Cu–Fe–S intermediate solid-solution. Late-stage, moderately oxidizing fluids may strongly alter the primary sulfide mineralization in immiscible sulfide deposits (*e.g.*, Pasteris 1984).

This study is based on a small number of samples from only two regions in the Duluth Complex. It is significant, however, that such strong mineralogical distinctions are recognized in two troctolitic bodies only about 25 km apart. Each body in turn represents multiple intrusions (*e.g.*, Tyson & Chang 1984), so that further documentation is needed on the mineralogical changes even within the bodies. For instance, at least minor amounts of magnetite occur in drill cores from other portions of the Minnamax deposit (E. Ripley & S. Mills 1984, pers. comm.). It would be useful to make a direct comparison of the mineralogy of the coexisting oxide and sulfide phases in several portions of the Minnamax body and to monitor how they change with depth.

ACKNOWLEDGEMENTS

The author thanks the following for supplying samples and information and for granting permission to publish these data: S.N. Watowich and J.B. Malcolm of Amax (Minnamax samples) and M.L. Boucher of the U.S. Bureau of Mines, Minneapolis (Inco samples). She also benefited from discussions with and suggestions from colleagues doing independent projects in the Complex, especially Norman Grant, Edward Ripley, Paul Weiblen, Christopher Chalokwu and Sarah Mills. Donald Lindsley and an anonymous reviewer are thanked for their comments on an earlier draft of the paper. Of particular help was Donald Lindsley's suggested constraints on interpreting suites where ilmenite occurs without titaniferous magnetite. The author, however, accepts full responsibility for all data and interpretations. This work was funded in part by NSF grant EAR-8025255; the support of the Research Corporation also is gratefully acknowledged.

REFERENCES

ALBEE, A.L. & RAY, L. (1970): Correction factors for electron probe microanalysis of silicates, oxides, carbonates, phosphates and sulfates. *Anal. Chem.* **42**, 1408-1414.

BARTON, P.B. & SKINNER, B.J. (1979): Sulfide mineral stabilities. *In* Geochemistry of Hydrothermal Ore Deposits (H.L. Barnes, ed.). John Wiley & Sons, New York.

BENCE, A.E. & ALBEE, A.L. (1968): Empirical correction factors for the electron microanalysis of silicates and oxides. *J. Geol.* **76**, 382-403.

BONNICHSEN, B. (1972a): Sulfide minerals in the Duluth Complex. *In* Geology of Minnesota: A Centennial Volume (P.K. Sims & G.B. Morey, eds.). Minnesota Geol. Surv. Spec. Vol., Minneapolis, Minn.

______ (1972b): Southern part of Duluth Complex. *In* Geology of Minnesota: A Centennial Volume (P.K. Sims & G.B. Morey, eds.). Minnesota Geol. Surv. Spec. Vol. Minneapolis, Minn.

______ (1974): Copper and nickel resources in the Duluth Complex, northeastern Minnesota. *Minn. Geol. Surv., Inf. Cir.* **10.**

Boucher, M.L. (1975): Copper–nickel mineralization in a drill core from the Duluth Complex of northern Minnesota. *U.S. Bur. Mines Rep. Invest.* **8084.**

Bowles, J.F.W. (1977): A method of tracing the temperature and oxygen-fugacity histories of complex magnetite–ilmenite grains. *Mineral. Mag.* **41,** 103-109.

Buchanan, D.L. & Nolan, J. (1979): Solubility of sulfur and sulfide immiscibility in synthetic tholeiitic melts and their relevance to Bushveld-Complex rocks. *Can. Mineral.* **17,** 483-494.

Buddington, A.F. & Lindsley, D.H. (1964): Iron-titanium oxide minerals and synthetic equivalents. *J. Petrology* **5,** 310-357.

Chou, I-ming (1978): Calibration of oxygen buffers at elevated P and T using the hydrogen fugacity sensor. *Amer. Mineral.* **63,** 690-703.

Copper, R.W., Morey, G.B. & Weiblen, P.W. (1978): Topographic and aeromagnetic lineaments and their relationship to bedrock geology in a glaciated Precambrian terrane, northeastern Minnesota. *In* Proc. Third Int. Conf. Basement Tectonics (D.W. O'Leary & J.L. Earle, eds.). Basement Tectonics Committee Inc., Denver, Colorado.

Craig, J.R. & Scott, S.D. (1974): Sulfide phase equilibria. *In* Sulfide Mineralogy (P.H. Ribbe, ed.). *Mineral. Soc. Amer., Rev. Mineral.* **1,** CS1-110.

Eugster, H.P. & Wones, D.R. (1962): Stability relations of the ferruginous biotite, annite. *J. Petrology* **3,** 82-125.

Garrison, J.R. & Taylor, L.A. (1981): Petrogenesis of pyroxene–oxide intergrowths from kimberlite and cumulate rocks: co-precipitation or exsolution? *Amer. Mineral.* **66,** 723-740.

Grant, N.K. & Molling, P.A. (1981): A strontium isotope and trace element profile through the Partridge River troctolite, Duluth Complex, Minnesota. *Contr. Mineral. Petrology* **77,** 296-305.

Haggerty, S.E. (1976): Opaque mineral oxides in terrestrial igneous rocks. *In* Oxide Minerals (D. Rumble III, ed.). *Mineral. Soc. Amer., Rev. Mineral.* **3,** Hg101-300.

Hammond, P.A. & Taylor, L.A. (1982): The ilmenite/titano-magnetite assemblage: kinetics of re-equilibration. *Earth Planet. Sci. Lett.* **61,** 143-150.

Hardyman, R.F. (1969): *The Petrography of a Section of the Basal Duluth Complex, St. Louis County, Northeastern Minnesota.* M.S. thesis, Univ. Minnesota, Minneapolis, Minn.

Haughton, D.R., Roeder, P.L. & Skinner, B.J. (1974): Solubility of sulfur in mafic magmas. *Econ. Geol.* **69,** 451-467.

Ishihara, S. (1981): The granitoid series and mineralization. *Econ. Geol. 75th Anniv. Vol.,* 458-484.

Lindsley, D.H. (1976): Experimental studies of oxide minerals. *In* Oxide Minerals (D. Rumble III, ed.). *Mineral. Soc. Amer., Rev. Mineral.* **3,** L61-88.

______ & Spencer, K.J. (1982): Fe–Ti oxide geothermometry: reducing analyses of coexisting Ti-magnetite (Mt) and ilmenite (Ilm). *Trans. Amer. Geophys. Union* **63,** 471 (abstr.).

Mainwaring, P.R. & Naldrett, A.J. (1977): Country-rock assimilation and the genesis of Cu–Ni sulfides in the Water Hen intrusion, Duluth Complex, Minnesota. *Econ. Geol.* **72,** 1269-1284.

Oliver, G.J.H. (1978): Ilmenite–magnetite geothermometry and oxygen barometry in granulite and amphibolite facies gneisses from Doubtful Sound, Fiordland, New Zealand. *Lithos* **11,** 147-153.

Pasteris, J.D. (1984): Further interpretation of the Cu–Fe–Ni sulfide mineralization in the Duluth Complex, northeastern Minnesota. *Can. Mineral.* **22,** 39-53.

Pedersen, A.K. (1979a): A shale buchite xenolith with Al-armalcolite and native iron in a lava from Asuk, Disko, central west Greenland. *Contr. Mineral. Petrology* **69,** 83-94.

______ (1979b): Basaltic glass with high-temperature equilibrated immiscible sulphide bodies with native iron from Disko, central west Greenland. *Contr. Mineral. Petrology* **69,** 394-407.

Phinney, W.C. (1972): Northwestern part of Duluth Complex. *In* Geology of Minnesota: A Centennial Volume (P.K. Sims & G.B. Morey, eds.). Minnesota Geol. Surv. Spec. Vol., Minneapolis, Minn.

Powell, R. & Powell, M. (1977): Geothermometry and oxygen barometry using coexisting iron-titanium oxides: a reappraisal. *Mineral. Mag.* **41,** 257-263.

Rao, B.V. & Ripley, E.M. (1983): Petrochemical studies of the Dunka Road Cu-Ni deposit, Duluth Complex, Minnesota. *Econ. Geol.* **78,** 1222-1238.

Ripley, E.M. (1981): Sulfur isotopic studies of the Dunka Road Cu-Ni deposit, Duluth Complex, Minnesota. *Econ. Geol.* **76,** 610-620.

——— & Rao, B.V. (1980): Oxygen isotopic studies of the Dunka Road Cu-Ni deposit, Duluth Complex, Minnesota. *Geol. Soc. Amer. Abstr. Programs* **12**, 510.

Robie, R.A., Hemingway, B.S. & Fisher, J.R. (1978): Thermodynamic properties of minerals and related substances at 298.15 K and 1 bar (10^5 pascals) pressure and at higher temperatures. *U.S. Geol. Surv. Bull.* **1452.**

Shima, H. & Naldrett, A.J. (1975): Solubility of sulfur in an ultramafic melt and the relevance of the system Fe–S–O. *Econ. Geol.* **70**, 960-967.

Spencer, K.J. & Lindsley, D.H. (1981): A solution model for coexisting iron–titanium oxides. *Amer. Mineral.* **66**, 1189-1201.

Stormer, J.C., Jr. (1982): The recalculation of multicomponent Fe–Ti oxide analyses for geothermometry: a quasi-thermodynamic model. *Trans. Amer. Geophys. Union* **63**, 471 (abstr.).

Toulmin, P., III & Barton, P.B., Jr. (1964): A thermodynamic study of pyrite and pyrrhotite. *Geochim. Cosmochim. Acta* **28**, 641-671.

Tyson, R.M. & Chang, L.L.Y. (1984): The petrology and sulfide mineralization of the Partridge River troctolite, Duluth Complex, Minnesota. *Can. Mineral.* **22**, 23-38.

Watowich, S.N. (1978): A preliminary geological view of the MINNAMAX copper–nickel deposit in the Duluth Gabbro. *Proc. 51st Ann. Meet. Minn. Sect. AIME, 39th Ann. Mining Symp.,* 19-1 to 19-11.

Weiblen, P.W. & Morey, G.B. (1976): Textural and compositional characteristics of sulfide ores from the basal contact zone of the South Kawishiwi intrusion, Duluth Complex, northeastern Minnesota. *Proc. 37th Ann. Mining Symp. (Minn. Geol. Surv. Reprint Ser.,* **32**), 22-1 to 22-24.

——— & ——— (1980): A summary of the stratigraphy, petrology, and structure of the Duluth Complex. *Amer. J. Sci.* **280A**, 88-133.

White, R.W. (1966): Ultramafic inclusions in basaltic rocks from Hawaii. *Contr. Mineral. Petrology* **12**, 245-314.

Whitney, J.A. (1984): Fugacities of sulfurous gases in pyrrhotite-bearing silicic magmas. *Amer. Mineral.* **69**, 69-78.

——— & Stormer, J.C., Jr. (1983): Igneous sulfides in the Fish Canyon Tuff and the role of sulfur in calc-alkaline magmas. *Geology* **11**, 99-102.

Received February 6, 1984, revised manuscript accepted July 31, 1984.